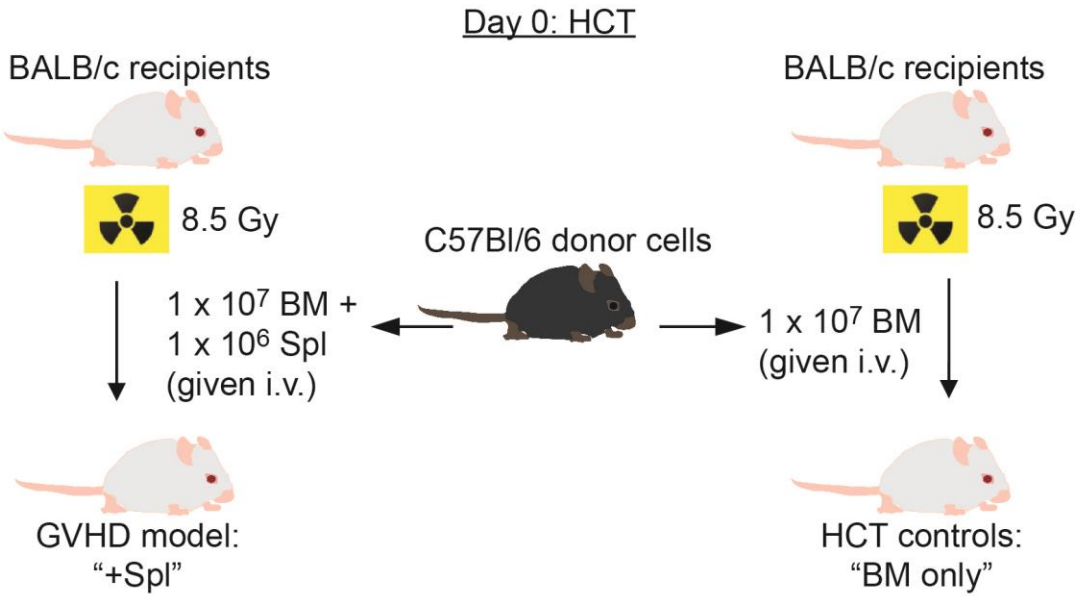

Day +12: Start ENTO or Placebo chow.

Day +19: Collect plasma for PK studies.

Throughout study:
Monitor survival and weight;
Obtain masked clinical scores of eye pathology and alopecia;
Assess immune cell reconstitution by flow cytometry;
Collect tissues from mice reaching humane endpoints.

Study endpoint (Day +120):
Collect tissues from surviving mice;
Masked histopathological analysis of skin from all mice.

Supplemental Figure 1. GVHD animal model and ENTO administration. (**A**) BALB/c recipient mice (*n*=10 per treatment group) were lethally irradiated (8.5 Gy) and then transplanted i.v. with 1 x 10^7 T cell-depleted C57BL/6 bone marrow cells alone (control HCT = "BM only"), or with 1 x 10^7 T cell-depleted C57BL/6 bone marrow cells plus 1 x 10^6 C57BL/6 splenocytes (develop GVHD = "+Spl"). On Day +12 after HCT, recipient mice were started on chow formulated with ENTO at a concentration of 0.06% or 0.02%, or with Placebo. Mice were evaluated for various disease criteria during the study, as described.

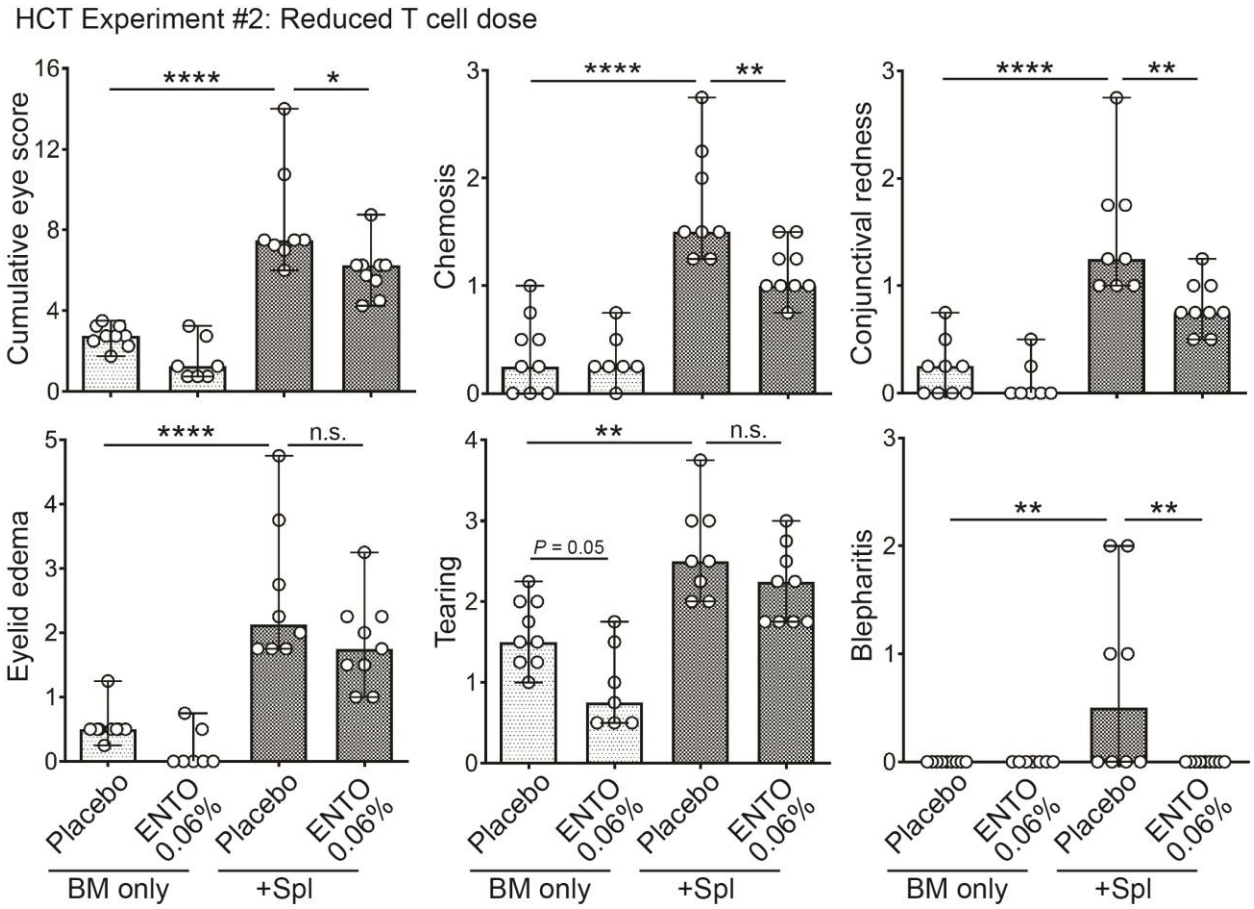

Supplemental Figure 2. ENTO improves clinical eye scores in GVHD mice receiving a reduced donor T cell dose. Mice (*n* = 7-9/group) in an independent HCT experiment using a reduced dose of donor T cells were evaluated for various clinical manifestations of eye pathology by an expert, masked investigator 4 wks following HCT as described in **Figure 2**. Each symbol in a particular graph represents the sum clinical scores of the right + left eye of a single mouse. Cumulative clinical eye scores for individual mice were determined by summing the scores for chemosis, conjunctival redness, eyelid edema, and tearing. Bars indicate the median (±range). Statistical analysis was performed by One-way ANOVA with Tukey's multiple comparisons test (GraphPad Prism). ****, $P < 0.0001$; **, $P < 0.01$; *, $P < 0.05$; n.s., not significant.

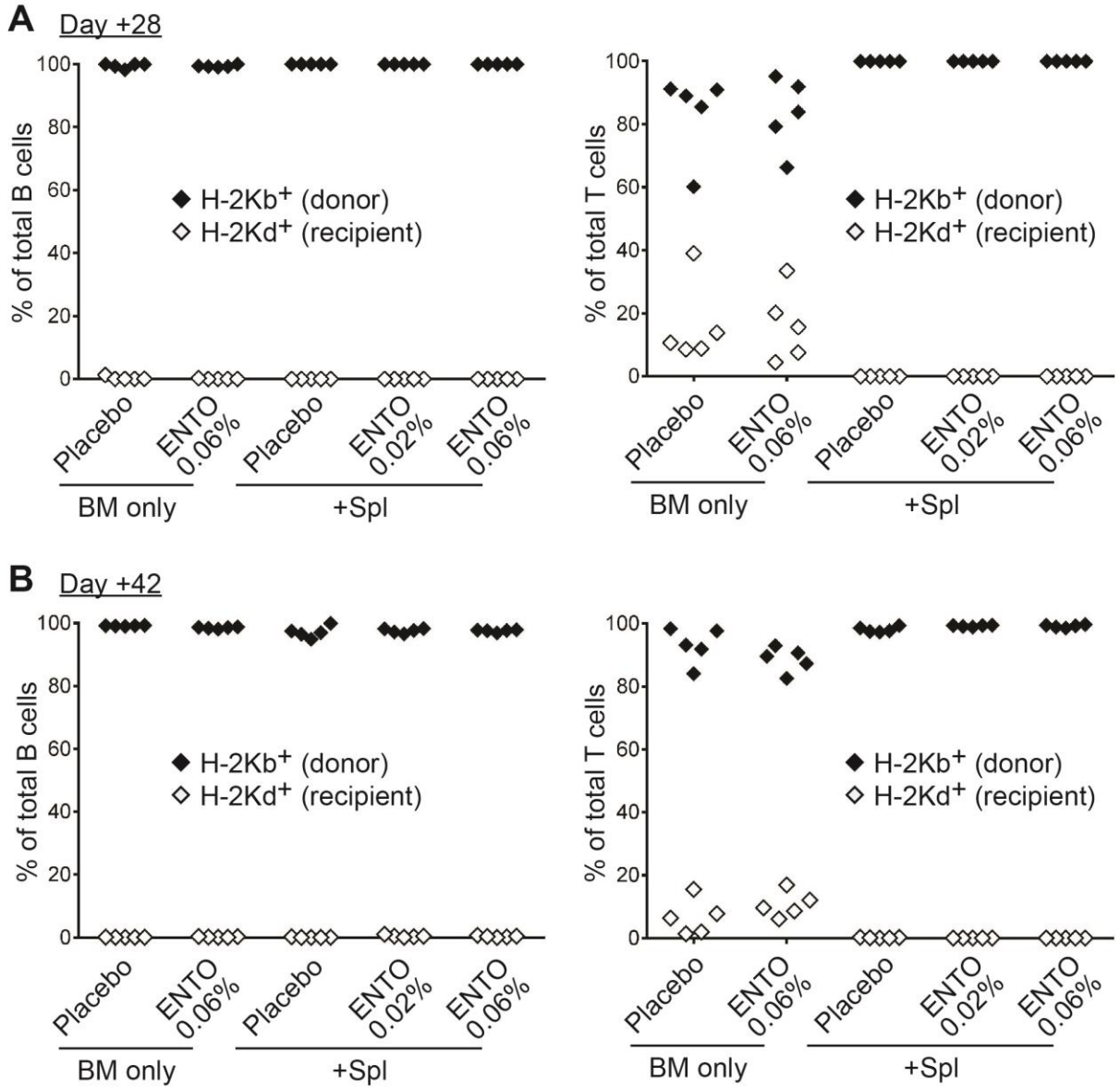

Supplemental Figure 3. +Spl mice were completely engrafted with donor lymphocytes. Lymphocyte allograft chimerism in HCT mice was assessed by flow cytometry on Day +28 **(A)** and Day +42 **(B)**. Each mouse is represented by both a filled symbol and an open symbol, defined as follows: The frequencies of donor cells (C57BL/6, H-2Kb$^+$ MHC haplotype, filled symbols) and recipient cells (BALB/c, H-2Kd$^+$ MHC haplotype, open symbols) for each lymphocyte subset out of the total are as indicated (B cells, left panels; T cells, right panels). All mice in each HCT group (*n* = 9-10/group) are represented either on Day +28 or on Day +42.

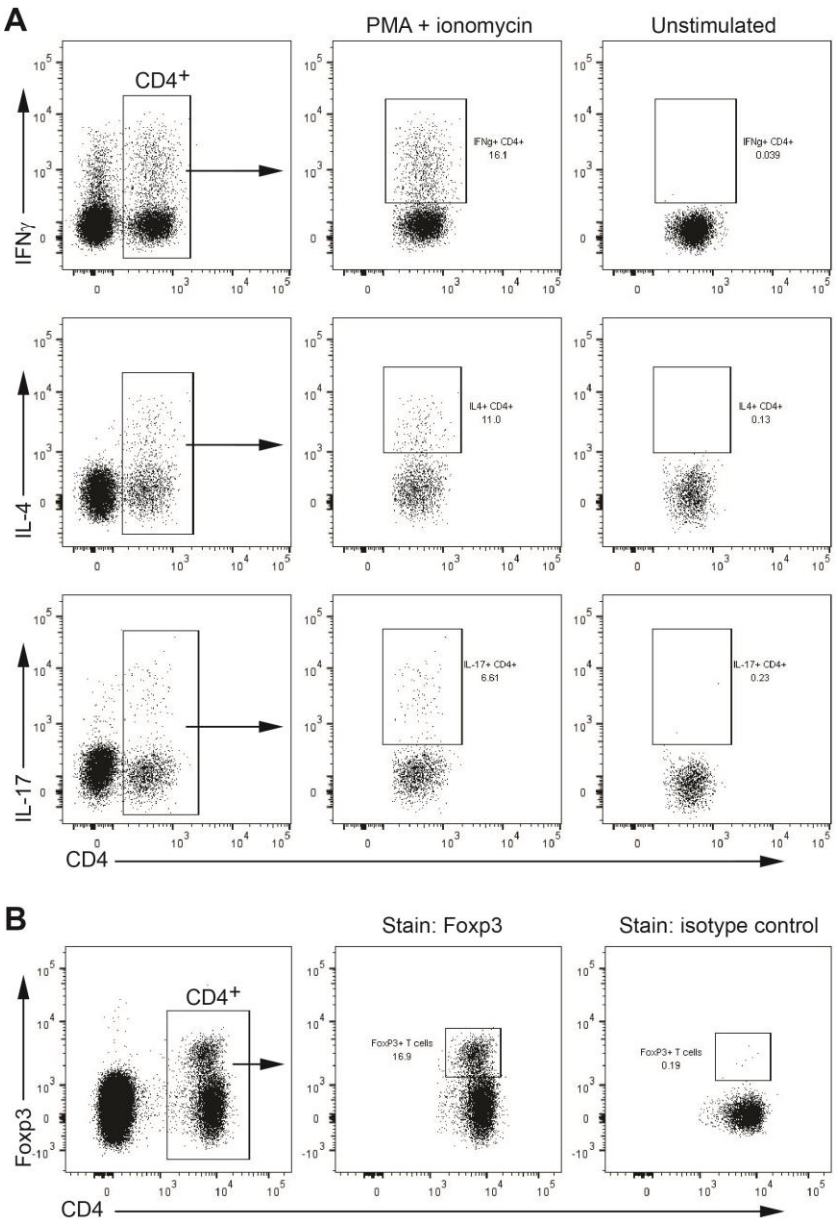

Supplemental Figure 4. Representative flow cytometry plots showing cytokine production, Foxp3 expression, and gating strategy for the Th1, Th2, Th17 and Treg subsets. (A) Flow cytometry plots of splenocytes from representative mice cultured in the presence or absence of PMA and ionomycin for 5h and then stained for surface CD4 and intracellularly for IFNγ (upper panels), IL-4 (middle panels), or IL-17 (lower panels). The gate used to identify $CD4^+$ T cells is indicated in the panels at left. The gates shown in the center panels were used to determine the frequency of cytokine-producing cells, set according to the negative cytokine staining for unstimulated cells (right panels). **(B)** Flow cytometry plots of splenocytes a representative mouse stained for surface CD4 and intracellularly for Foxp3. The gate used to identify $CD4^+$ T cells is indicated in the panel at left. The gate shown in the center panel was used to determine the frequency of $Foxp3^+$ cells, set according to the negative staining using an isotype control Ab (right panel).

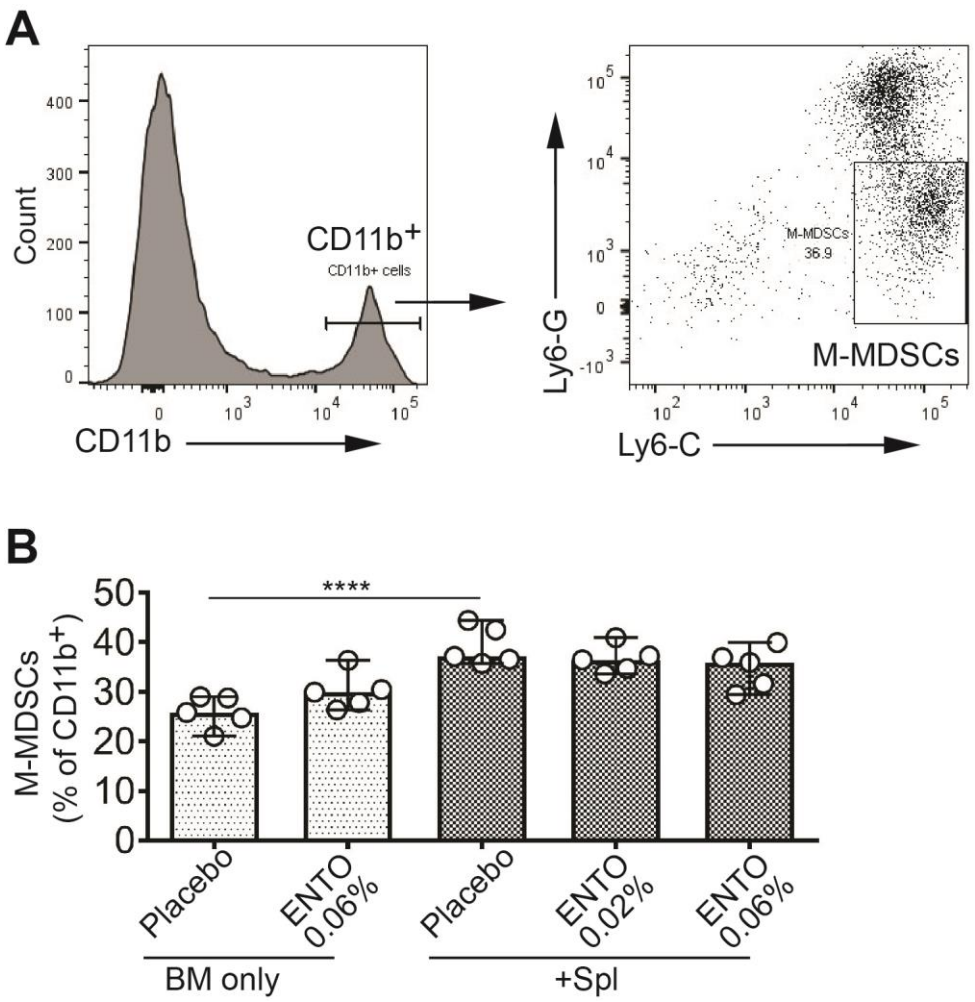

Supplemental Figure 5. Monocytic myeloid-derived suppressor cell (M-MDSC) frequency is similar between +Spl GVHD mouse groups. (A) Splenocytes from a representative mouse surface stained for CD11b, Ly6-C and Ly6-G. M-MDSCs were identified as CD11b+ cells (left panel) that were also positive for Ly6-C and negative for Ly6-G (gated region in right panel). **(B)** Frequency of M-MDSCs within total $CD11b^+$ splenocytes from the mice from all groups represented in **Figure 5**. Bars indicate the median (±range). Statistical analysis was performed by One-way ANOVA with Tukey's multiple comparisons test (GraphPad Prism). ****, $P < 0.0001$.

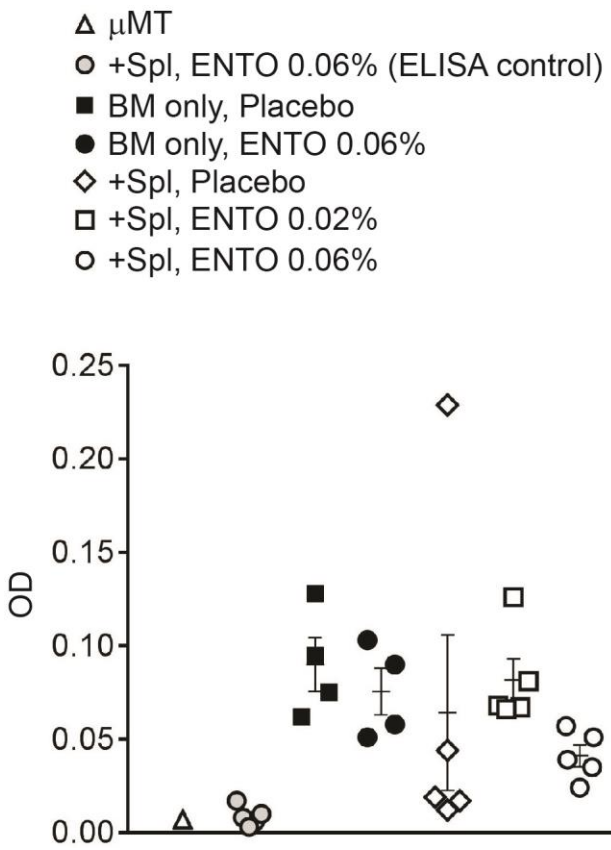

Supplemental Figure 6. Natural IgM antibodies against vaccinia virus (VV) are present in all experimental HCT groups. Day +42 plasma samples from BM only (*n* = 4 each) and +Spl groups (*n* = 5 each) were serially diluted and subjected to ELISA using VV-coated ELISA plates. Shown are the results from plasma samples diluted at 1:400. Error bars indicate the mean ±SEM. Plasma from a μMT mouse, which are genetically incapable of producing mature B cells and thus lack plasma antibodies, was used as a negative control (triangle). As an additional control to show that natural IgM was specific for VV, ELISA wells not coated with VV were used for some samples (ELISA control, gray-filled circles).

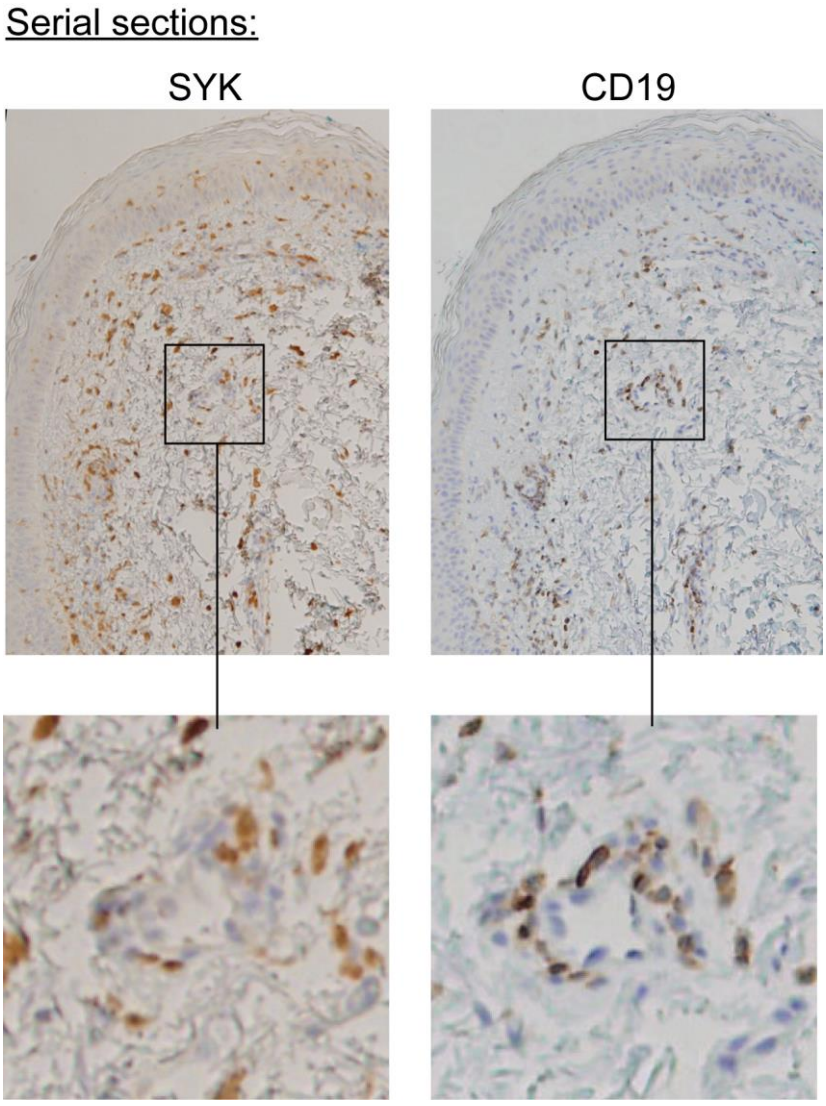

Supplemental Figure 7. SYK+ cells are abundant in the dermis of lichenoid skin lesions from chronic GVHD patients. Immunohistochemistry was performed on FFPE sections of lichenoid skin lesions obtained from a patient with chronic GVHD. The sections were stained either with anti-SYK Ab (left panels) or anti-CD19 Ab (right panels), each indicated by brown color, and counterstained with hematoxylin (blue color) as described in the Methods section. Lower panels show representative regions from the upper panels that have been enlarged to highlight the localization and general morphology of SYK+ or CD19+ cells.